PHOTONICS Research

Dry-etched ultrahigh-Q silica microdisk resonators on a silicon chip

Jiaxin Gu,[1] Jie Liu,[1] Ziqi Bai,[1] Han Wang,[1] Xinyu Cheng,[1] Guanyu Li,[1] Menghua Zhang,[1] Xinxin Li,[1] Qi Shi,[1] Min Xiao,[1,2] and Xiaoshun Jiang[1,*]

[1]National Laboratory of Solid State Microstructures, College of Engineering and Applied Science and School of Physics, Nanjing University, Nanjing 210093, China
[2]Department of Physics, University of Arkansas, Fayetteville, Arkansas 72701, USA
*Corresponding author: jxs@nju.edu.cn

Received 19 October 2020; revised 6 February 2021; accepted 11 February 2021; posted 12 February 2021 (Doc. ID 412840); published 22 April 2021

We demonstrate the fabrication of ultrahigh quality (Q) factor silica microdisk resonators on a silicon chip by inductively coupled plasma (ICP) etching. We achieve a dry-etched optical microresonator with an intrinsic Q factor as high as 1.94×10^8 from a 1-mm-diameter silica microdisk with a thickness of 4 μm. Our work provides a chip-based microresonator platform operating in the ultrahigh-Q region that will be useful in nonlinear photonics such as Brillouin lasers and Kerr microcombs.

https://doi.org/10.1364/PRJ.412840

1. INTRODUCTION

Optical microresonators [1], owing to their long photon storage time in small spatial volumes, enable strong enhancement of optical interactions, especially in the generation of soliton microcombs [2,3]. Specifically, the need to enhance desired nonlinear processes has motivated the development of different material platforms in improving the Q factors of such microresonators. In recent years, there has been progress made in many chip-based material platforms, such as silica [4–7], silicon nitride [8–12], lithium niobate [13,14], and others [15–22]. Among them, the chip-based silica microresonators in the forms of microtoroid, microsphere, as well as microdisk exhibit the highest Q factors [4–7]. Compared to the microtoroid and microsphere resonators, the silica microdisk resonators are more widely used for Brillouin lasers [5] and Kerr soliton microcombs [23] owing to the controllabilities of the free spectral range (FSR) and dispersion in such structures with the diameter, wedge angle, as well as thickness [23]. Also, due to the low material dispersion and ultrahigh Q factor, Kerr soliton microcombs with a repetition rate as low as 1.86 GHz have been achieved using a 35-mm-diameter microdisk resonator [24]. However, due to the fabrication limitations, such ultrahigh-Q silica microdisk resonators have only been obtained by using a chemical wet-etching technique [5,7]. In that work, extended hydrofluoric acid (HF) wet etching was performed to remove the "foot" region of the silica layer induced by the wet etching, which makes the diameter of the fabricated microresonator much smaller than the initial design [5].

In a previous work, a dry-etched silica microdisk resonator [25] with an optical Q factor of 2.4×10^7 was fabricated and used for visible Kerr microcomb generation by controlling the dispersion with the wedge angle [26]. Very recently, full integration of silica-based optical resonators with a waveguide using one material platform has been presented [27]. However, silica optical microresonators based on dry etching have never achieved the same ultrahigh-Q ($Q > 100$ million) values as demonstrated by those that are chemically etched.

In this work, by optimizing the fabrication process, we have obtained ultrahigh-Q silica microdisk resonators on a silicon chip by employing an inductively coupled plasma (ICP) dry-etching technique. The intrinsic optical Q factor as high as 194 million is demonstrated by fabricating a 1-mm-diameter silica microdisk resonator with a thickness of 4 μm. To the best of our knowledge, this is the first report of chip-based ultrahigh-Q silica microresonators fabricated by dry etching.

2. FABRICATION AND CHARACTERIZATION

Our standard fabrication process is similar to that shown in our previous work [25,26,28]. Compared with the HF wet etching [5], the dry-etching process usually produces larger sidewall roughness and increases the difficulty in removing photoresist, which significantly affects the Q factors of the microresonators. In this work, by improving the fabrication process such as reducing the sidewall roughness and adding a silicon layer to make the residual photoresist on top surface of the silica microdisk be easily removed, we have boosted the dry-etched silica microresonators into the ultrahigh-Q region.

So far, the optical Q factor of the chip-based silica microdisk resonator is limited by the scattering losses induced by the

surface roughness of the microresonator. For the dry-etched microdisk resonators, the sidewall roughness predominantly results from two pattern-transfer steps: lithography-induced roughness and dry-etch-induced roughness. During photolithography, we optimized the hard-bake temperature and duration time of the patterned photoresist to obtain a smooth sidewall of the mask. For the dry-etching process, we employed an etching system based on neutral loop discharge (NLD) plasmas (ULVAC, NLD 570) [29]. These NLD plasmas tend to have high plasma density with a relatively low electron temperature [30], which lowers the substrate temperature and thus reduces the difficulty in subsequently removing the photoresist. This is of great importance, particularly for the long-time plasma etching in this work. During the ICP etching, CF_4 is used as the main etch gas with a small amount of SF_6. In our experiment, due to the limited selectivity between the photoresist and the silica layer, the etching recipe such as the flow rate of the SF_6 (40.0 sccm) and CF_4 (3.0 sccm) (sccm, standard cubic centimeters per minute) as well as the ICP power (400 W) is specifically adjusted to make a balance between the etching rate and the selectivity. Figures 1(a) and 1(b) show the optical and scanning electron microcopy images of the dry-etched silica microdisk with a wedge angle of around 35°.

Owing to the hard bake of the photoresist and long-time ICP etching, photoresist removal will be a significant challenge by just using the photoresist remover and piranha solution. Here we employed a new method that involves deposition of a thin a-Si layer before lithography to isolate the silica layer from the photoresist [Fig. 2(a)]; the a-Si layer is around 100 nm in thickness. It should be noted that the a-Si layer and the organic materials adhered on it can be removed during the XeF_2 dry etching [Fig. 2(e)]. Usually, the undercut for the fabricated silica microdisk resonator is 30–80 μm to avoid the coupling of the optical mode to the silicon pillar. After the XeF_2 dry etching, the silica microdisks are annealed at 1000°C in an oxygen ambient to drive down the water content in the silicon oxide

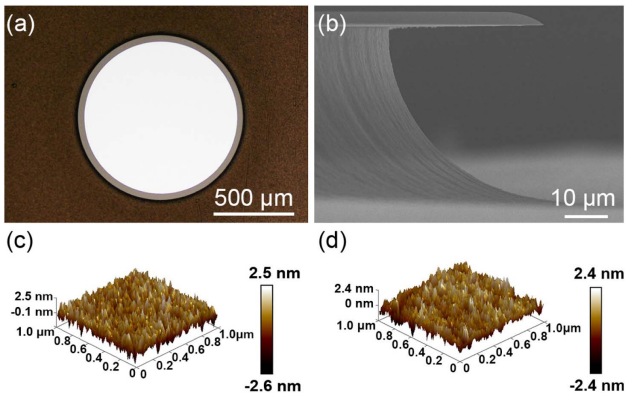

Fig. 1. Typical images and atomic force microscope measurement of the ultrahigh-Q wedged silica microdisk (diameter: 1 mm, thickness: 4 μm). (a) Optical micrograph showing the top view of the microdisk. (b) Side-view scanning electron microcopy image of the wedged silica microdisk. (c) 3D AFM scan of the top surface with RMS roughness of 0.72 nm and correlation length of 30 nm. (d) 3D AFM scan of the sidewall with RMS roughness of 0.67 nm and correlation length of 20 nm.

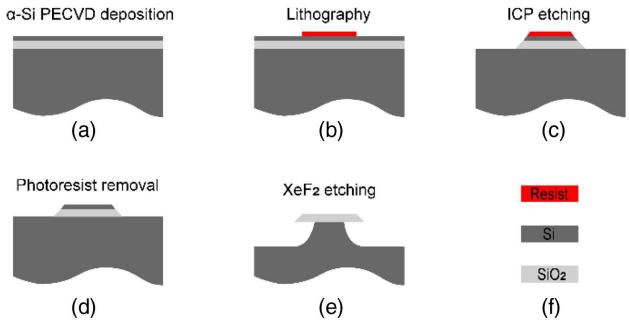

Fig. 2. Fabrication process flow for the dry-etched wedged silica microdisk resonators. (a) Thermally grown silica layer on a silicon chip and subsequent deposition of an a-Si layer by plasma enhanced chemical vapor deposition (PECVD). (b) Pattern definition by UV lithography. (c) ICP etching to transfer the mask pattern to the silica layer. (d) Photoresist removal. (e) XeF_2 etching to form the silicon pillar and remove the a-Si layer. (f) Colors used to indicate different materials.

layer and the residual polymer on sidewalls formed during the ICP dry-etching process.

To characterize the silica microdisk resonator, a tapered optical fiber is used to excite the optical modes of the microresonator via the evanescent wave [31]. We obtain the transmission spectrum by scanning an external semiconductor laser at the 1550 nm wavelength across the resonance frequency. By adjusting the distance between the taper fiber and the resonator, the resonator can be undercoupled to avoid the thermo-optic effect [32], which makes the measured value close to the intrinsic optical Q factor. Further adjusting the distance between the taper fiber and the resonator, the critical coupling and overcoupling regimes can also be accessed. During the measurement, the optical modes are calibrated using a fiber Mach–Zehnder interferometer.

For comparison, we have also fabricated wedged silica microdisk resonators using a different process. As shown in Fig. 3, the first chip (chip 1) was fabricated using the standard process, while the other one (chip 2) employed an additional a-Si layer.

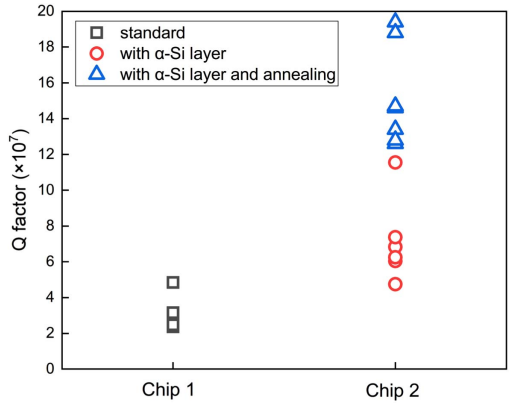

Fig. 3. Comparison of intrinsic Q factors of samples from two distinct chips fabricated using different processes. Chip 1, standard process; Chip 2, optimized standard process by adding an a-Si layer, with (blue triangles) and without (red cycles) the additional thermal annealing process.

Chip 2 was also used to compare the effect of additional thermal annealing. All of the wedged silica microdisks have the same designed size and thickness (diameter: 1 mm, thickness: 4 μm). Both the a-Si layer and the additional thermal annealing have the tendency to achieve higher optical Q factors as shown in Fig. 3. As shown in Fig. 4(a), we finally obtain an intrinsic Q factor of 193.9 million from a dry-etched wedged silica microdisk with an FSR of 65.4 GHz. Mode splitting in the transmission spectrum was induced by the backscattering of light from surface roughness [33]. We attribute the large mode splitting to the relatively large Q factor and small mode volume for our dry-etched microresonator [34]. The sinusoidal curve accompanying the spectrum is a calibration scan using a fiber Mach–Zehnder interferometer with an FSR of 0.192 MHz.

To further confirm the measured Q factors of the microresonators, accurate measurement using the ringing method [35,36] was also performed to minimize the influence of thermal effects and laser frequency noise. The laser excites the optical mode, which results in the interference between the delayed light from the resonator and the direct transmitted pump laser. Figure 4(b) shows the ringing curve of the optical mode in Fig. 4(a). The theoretical fit shows an intrinsic Q factor of 196.2 million, which matches quite well with the Lorentzian fit in Fig. 4(a). Particular attention should be paid to the fact that the Q factor is even higher than that for a chemically etched analogue with the same diameter and thickness [5].

To show the nonlinear optical application, we have demonstrated the optical parametric oscillation using a dry-etched silica microdisk resonator with an intrinsic Q factor and loaded Q factor of 100.8 million and 74.4 million, respectively. Figure 5 shows the generated sidebands' power versus input pump power, which gives a threshold power as low as 1.63 mW.

To evaluate the surface roughness of the fabricated microdisk resonators, we have performed atomic force microscope (AFM) measurement. As shown in Figs. 1(c) and 1(d), the root-mean-squared (RMS) roughness is 0.72 nm for the top surface and 0.67 nm for the sidewall. The relatively larger roughness of the top surface may be attributed to the residual photoresist or silicon. The roughness of the sidewall is similar to the measured value of the wet-etched silica microdisk resonator [5]. Also, the autocorrelation lengths for the top surface and the sidewall are around 20 nm and 30 nm, respectively, which are much smaller than that obtained from wet etching [5]. In the future, the optical Q factor can be further increased by optimizing the fabrication process such as the removal of the photoresist on the top surface of the microresonator.

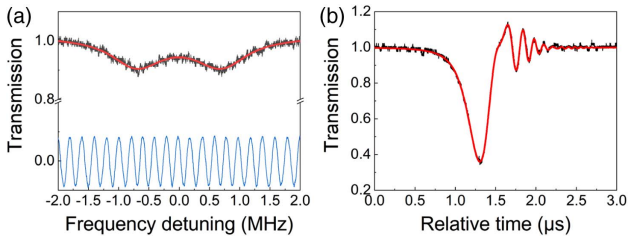

Fig. 4. Characterization of the ultrahigh-Q wedged silica microdisk. (a) Spectral scan for the case of a Q factor of 193.9 million with a full width at half-maximum (FWHM) of 0.996 MHz. The doublet feature in the transmission spectrum is caused by the mode coupling between the clockwise and counterclockwise propagation modes [33]. The sinusoidal curve accompanying the spectrum is a calibration scan using a fiber Mach–Zehnder interferometer. (b) Experimental ringing curve of the optical mode in (a) and its theoretical fit with a Q factor of 196.2 million.

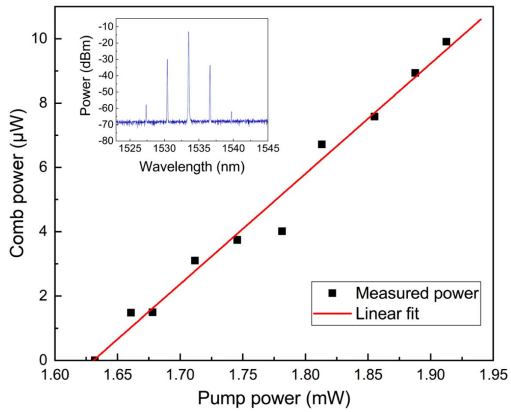

Fig. 5. Sidebands' power versus input pump power. The measured threshold is 1.63 mW for the silica microdisk. The inset shows the optical spectrum with the pump power of 1.66 mW.

3. CONCLUSION

In conclusion, ultrahigh-Q (1.94×10^8) silica microdisk resonators on a silicon chip have been successfully demonstrated by dry etching. Such dry-etched devices will be useful for Brillouin lasers with precise FSR control. The fabrication process will also be applicable to multiwedge resonators [37] for broadband dispersion engineering by only controlling the dry-etching process with photolithography and ultralow-loss delay line on chip [38]. Our method also paves the way for the on-chip integration of ultrahigh-Q microresonators with the bus waveguides within silica material.

Funding. National Key Research and Development Program of China (2016YFA0302500, 2017YFA0303703); National Natural Science Foundation of China (NFSC) (61922040, 11621091); Fundamental Research Funds for the Central Universities (021314380149).

Acknowledgment. The authors thank Jiayu Zhang, Hongyu Yang, and Kuo Yang for assistance with AFM measurement.

Disclosures. The authors declare no conflicts of interest.

REFERENCES

1. K. J. Vahala, "Optical microcavities," Nature **424**, 839–846 (2003).
2. T. J. Kippenberg, A. L. Gaeta, M. Lipson, and M. L. Gorodetsky, "Dissipative Kerr solitons in optical microresonators," Science **361**, eaan8083 (2018).
3. P. Del'Haye, A. Schliesser, O. Arcizet, T. Wilken, R. Holzwarth, and T. Kippenberg, "Optical frequency comb generation from a monolithic microresonator," Nature **450**, 1214–1217 (2007).
4. D. Armani, T. Kippenberg, S. Spillane, and K. Vahala, "Ultra-high-Q toroid microcavity on a chip," Nature **421**, 925–928 (2003).

5. H. Lee, T. Chen, J. Li, K. Y. Yang, S. Jeon, O. Painter, and K. J. Vahala, "Chemically etched ultrahigh-Q wedge-resonator on a silicon chip," Nat. Photonics **6**, 369–373 (2012).
6. J.-B. Jager, V. Calvo, E. Delamadeleine, E. Hadji, P. Noé, T. Ricart, D. Bucci, and A. Morand, "High-Q silica microcavities on a chip: from microtoroid to microsphere," Appl. Phys. Lett. **99**, 181123 (2011).
7. L. Wu, H. Wang, Q. Yang, Q. Ji, B. Shen, C. Bao, M. Gao, and K. Vahala, "Greater than one billion Q factor for on-chip microresonators," Opt. Lett. **45**, 5129–5131 (2020).
8. Y. Xuan, Y. Liu, L. T. Varghese, A. J. Metcalf, X. Xue, P.-H. Wang, K. Han, J. A. Jaramillo-Villegas, A. Al Noman, C. Wang, S. Kim, M. Teng, Y. J. Lee, B. Niu, L. Fan, J. Wang, D. E. Leaird, A. M. Weiner, and M. Qi, "High-Q silicon nitride microresonators exhibiting low-power frequency comb initiation," Optica **3**, 1171–1180 (2016).
9. D. T. Spencer, J. F. Bauters, M. J. Heck, and J. E. Bowers, "Integrated waveguide coupled Si_3N_4 resonators in the ultrahigh-Q regime," Optica **1**, 153–157 (2014).
10. X. Ji, F. A. Barbosa, S. P. Roberts, A. Dutt, J. Cardenas, Y. Okawachi, A. Bryant, A. L. Gaeta, and M. Lipson, "Ultra-low-loss on-chip resonators with sub-milliwatt parametric oscillation threshold," Optica **4**, 619–624 (2017).
11. M. H. Pfeiffer, J. Liu, A. S. Raja, T. Morais, B. Ghadiani, and T. J. Kippenberg, "Ultra-smooth silicon nitride waveguides based on the Damascene reflow process: fabrication and loss origins," Optica **5**, 884–892 (2018).
12. M. H. Pfeiffer, A. Kordts, V. Brasch, M. Zervas, M. Geiselmann, J. D. Jost, and T. J. Kippenberg, "Photonic Damascene process for integrated high-Q microresonator based nonlinear photonics," Optica **3**, 20–25 (2016).
13. M. Zhang, C. Wang, R. Cheng, A. Shams-Ansari, and M. Lončar, "Monolithic ultra-high-Q lithium niobate microring resonator," Optica **4**, 1536–1537 (2017).
14. A. Boes, B. Corcoran, L. Chang, J. Bowers, and A. Mitchell, "Status and potential of lithium niobate on insulator (LNOI) for photonic integrated circuits," Laser Photon. Rev. **12**, 1700256 (2018).
15. B. Hausmann, I. Bulu, V. Venkataraman, P. Deotare, and M. Lončar, "Diamond nonlinear photonics," Nat. Photonics **8**, 369–374 (2014).
16. M. Pu, L. Ottaviano, E. Semenova, and K. Yvind, "Efficient frequency comb generation in AlGaAs-on-insulator," Optica **3**, 823–826 (2016).
17. Z. Gong, A. Bruch, M. Shen, X. Guo, H. Jung, L. Fan, X. Liu, L. Zhang, J. Wang, J. Li, J. Yan, and H. X. Tang, "High-fidelity cavity soliton generation in crystalline AlN micro-ring resonators," Opt. Lett. **43**, 4366–4369 (2018).
18. D. J. Wilson, K. Schneider, S. Hönl, M. Anderson, Y. Baumgartner, L. Czornomaz, T. J. Kippenberg, and P. Seidler, "Integrated gallium phosphide nonlinear photonics," Nat. Photonics **14**, 57–62 (2020).
19. X. Lu, J. Y. Lee, S. Rogers, and Q. Lin, "Optical Kerr nonlinearity in a high-Q silicon carbide microresonator," Opt. Express **22**, 30826–30832 (2014).
20. L. Chang, W. Xie, H. Shu, Q.-F. Yang, B. Shen, A. Boes, J. D. Peters, W. Jin, C. Xiang, S. Liu, G. Moille, S.-P. Yu, X. Wang, K. Srinivasan, S. B. Papp, K. Vahala, and J. E. Bowers, "Ultra-efficient frequency comb generation in AlGaAs-on-insulator microresonators," Nat. Commun. **11**, 1331 (2020).
21. A. Biberman, M. J. Shaw, E. Timurdogan, J. B. Wright, and M. R. Watts, "Ultralow-loss silicon ring resonators," Opt. Lett. **37**, 4236–4238 (2012).
22. S. A. Miller, M. Yu, X. Ji, A. G. Griffith, J. Cardenas, A. L. Gaeta, and M. Lipson, "Low-loss silicon platform for broadband mid-infrared photonics," Optica **4**, 707–712 (2017).
23. X. Yi, Q.-F. Yang, K. Y. Yang, M.-G. Suh, and K. Vahala, "Soliton frequency comb at microwave rates in a high-Q silica microresonator," Optica **2**, 1078–1085 (2015).
24. M.-G. Suh and K. Vahala, "Gigahertz-repetition-rate soliton microcombs," Optica **5**, 65–66 (2018).
25. G. Li, P. Liu, X. Jiang, C. Yang, J. Ma, H. Wu, and M. Xiao, "High-Q silica microdisk optical resonators with large wedge angles on a silicon chip," Photon. Res. **3**, 279–282 (2015).
26. J. Ma, L. Xiao, J. Gu, H. Li, X. Cheng, G. He, X. Jiang, and M. Xiao, "Visible Kerr comb generation in a high-Q silica microdisk resonator with a large wedge angle," Photon. Res. **7**, 573–578 (2019).
27. C. Pyrlik, J. Schlegel, F. Böhm, A. Thies, O. Krüger, O. Benson, A. Wicht, and G. Tränkle, "Integrated thermal silica micro-resonator waveguide system with ultra-low fluorescence," IEEE Photon. Technol. Lett. **31**, 479–482 (2019).
28. X. Jiang, Q. Lin, J. Rosenberg, K. Vahala, and O. Painter, "High-Q double-disk microcavities for cavity optomechanics," Opt. Express **17**, 20911–20919 (2009).
29. T. Uchida, "Application of radio-frequency discharged plasma produced in closed magnetic neutral line for plasma processing," Jpn. J. Appl. Phys. **33**, L43–L44 (1994).
30. T. Uchida and S. Hamaguchi, "Magnetic neutral loop discharge (NLD) plasmas for surface processing," J. Phys. D **41**, 083001 (2008).
31. M. Cai, O. Painter, and K. J. Vahala, "Observation of critical coupling in a fiber taper to a silica-microsphere whispering-gallery mode system," Phys. Rev. Lett. **85**, 74–77 (2000).
32. T. Carmon, L. Yang, and K. J. Vahala, "Dynamical thermal behavior and thermal self-stability of microcavities," Opt. Express **12**, 4742–4750 (2004).
33. T. Kippenberg, S. Spillane, and K. Vahala, "Modal coupling in traveling-wave resonators," Opt. Lett. **27**, 1669–1671 (2002).
34. M. L. Gorodetsky, A. D. Pryamikov, and V. S. Ilchenko, "Rayleigh scattering in high-Q microspheres," J. Opt. Soc. Am. B **17**, 1051–1057 (2000).
35. A. A. Savchenkov, A. B. Matsko, V. S. Ilchenko, and L. Maleki, "Optical resonators with ten million finesse," Opt. Express **15**, 6768–6773 (2007).
36. C. Dong, C. Zou, J. Cui, Y. Yang, Z. Han, and G. Guo, "Ringing phenomenon in silica microspheres," Chin. Opt. Lett. **7**, 299–301 (2009).
37. K. Y. Yang, K. Beha, D. C. Cole, X. Yi, P. Del'Haye, H. Lee, J. Li, D. Y. Oh, S. A. Diddams, S. B. Papp, and K. J. Vahala, "Broadband dispersion-engineered microresonator on a chip," Nat. Photonics **10**, 316–320 (2016).
38. H. Lee, T. Chen, J. Li, O. Painter, and K. J. Vahala, "Ultra-low-loss optical delay line on a silicon chip," Nat. Commun. **3**, 867 (2012).